Vulpe, C. *et al.* (2014) ***Géotechnique Letters* 4**, 187–196, http://dx.doi.org/10.1680/geolett.14.00010

A generalised failure envelope for undrained capacity of circular shallow foundations under general loading

C. VULPE*, S. GOURVENEC* and M. POWER†

This paper presents a generalised failure envelope for the prediction of the undrained capacity of circular shallow foundations under general vertical, horizontal and moment (VHM) loading. Uniaxial capacities and failure envelopes under combined loading are presented for shallow circular foundations over a practical range of embedment ratio and soil strength heterogeneity. An approximating expression is proposed to describe the shape of the normalised VHM failure envelope as a function of foundation embedment ratio, normalised soil strength heterogeneity index and vertical load mobilisation.

KEYWORDS: bearing capacity; footings/foundations; offshore engineering

ICE Publishing: all rights reserved

NOTATION

A	cross-sectional plan area of the foundation
D	foundation diameter
d	skirt depth
d_{cV}, d_{cH}, d_{cM}	depth factors
E_u	undrained Young's modulus
H	horizontal load
H_{ult}	uniaxial horizontal capacity
k	undrained shear strength gradient
M	moment
M_{ult}	uniaxial moment capacity
N_{cV}, N_{cH}, N_{cM}	bearing capacity factors
s_u	undrained shear strength
s_{um}	undrained shear strength at the mudline
V	vertical load
V_{ult}	uniaxial vertical capacity
z	depth
γ'	effective unit weight
κ	soil heterogeneity index
v	Poisson's ratio

INTRODUCTION

General loading of foundation systems may arise from the combined actions of self-weight, inclined or eccentrically applied dead loads, operational or environmental loads. The capacity of foundations under general loading is a fundamental problem of geotechnical engineering and the advantage of failure envelope methods that explicitly account for independent load components over classical bearing capacity is widely acknowledged (Roscoe & Schofield, 1957; Butterfield & Ticof, 1979; Gottardi & Butterfield, 1993; Ukritchon *et al.*, 1998; Martin & Houlsby, 2001; Gourvenec & Randolph, 2003; Gourvenec & Barnett, 2011). Advantages of failure envelope methods over classical bearing capacity theory include

Manuscript received 12 February 2014; first decision 12 March 2014; accepted 14 July 2014.
Published online at www.geotechniqueletters.com on 19 August 2014.
*Centre for Offshore Foundation Systems & ARC Centre of Excellence for Geotechnical Science and Engineering, University of Western Australia, Perth, WA, Australia
†Fugro-TSM, Perth, WA 6000, Australia, formerly a student at University of Western Australia

- explicit consideration of (H, M/D,) interaction as opposed to linear superposition of load inclination and load eccentricity
- coupling of the horizontal and moment degrees of freedom for embedded foundations as opposed to a depth factor, the latter in effect leading to isotropic expansion of the failure envelope
- concurrent consideration of foundation geometry, embedment and soil strength profile as opposed to the superposition of independent factors
- provision for uplift resistance for skirted foundations at low vertical loads as opposed to the assumption of 'lift-off' under overturning moment at vertical loads less than half the ultimate uniaxial capacity ($V/V_{ult} \leq 0{\cdot}5$) implied by the effective area method (Meyerhof, 1953)
- an indication of the proximity to failure in terms of changes in individual load components as opposed to a reduction in vertical bearing pressure (Gourvenec & Barnett, 2011).

The failure envelope approach is not new (Roscoe & Schofield, 1957), and has been widely applied to bearing capacity problems (e.g. Butterfield & Ticof, 1979; Nova & Montrasio, 1991; Butterfield & Gottardi, 1994; Martin & Houlsby, 2001; Bransby & Randolph, 1998; Ukritchon *et al.*, 1998; Taiebat & Carter, 2000; Gourvenec & Randolph, 2003; Gourvenec, 2007a, 2007b; Bransby & Yun, 2009; Gourvenec & Barnett, 2011; Govoni *et al.*, 2011; Zhang *et al.*, 2011; Vulpe *et al.*, 2013; Mana *et al.*, 2013; Feng *et al.*, 2014).

Previous investigations have addressed plane strain and three-dimensional (3D) conditions, surface and embedded foundations, and uniform and linearly increasing shear strength profiles, but not comprehensively for all combinations. A summary of published work on failure envelopes for the undrained capacity of shallow foundations under general loading is shown in Table 1. Table 1 highlights the coverage and gaps in the knowledge base of undrained ultimate limit states under general vertical, horizontal and moment (VHM) loading for shallow foundations. A systematic study of embedded circular foundations across a range of soil strength heterogeneity is notably absent, and provided the motivation for this study.

This study addressed the undrained capacity of circular shallow foundations under general VHM loading. Expressions are presented to predict pure vertical, horizontal

Downloaded by [University Of Western Australia] on [15/11/15]. Copyright © ICE Publishing, all rights reserved.

Table 1. Summary of published work on undrained capacity of shallow foundations under general loading

Foundation geometry		Embedment		Interface condition		Soil strength kD/s_{um}	VHM expression	Method [a]	Reference
Strip	Circular/rectangular	Surface	Embedded	Unlimited tension	No tension				
+	—	+	—	+	+	≤12	—	NLA	Ukritchon *et al.* (1998)
+	—	+	—	+	—	6	+	FEA	Bransby & Randolph (1998)
+	—	—	+	+	—	0, 6	+	FEA/LUB	Bransby & Randolph (1999)
	C		+	+		0	+	EXP	Martin & Houlsby (2001) [b]
+	—	—	+	+	—	0, 200	—	FEA	Bransby & Yun (2009)
+	—	+	+	+	—	0, 200	+ [c]	FEA/LUB	Yun & Bransby (2007)
+	—	+	+	+	—	0	—	FEA	Gourvenec (2008)
+	—	+	+	+	—	≤6	+	FEA	Gourvenec & Barnett (2011)
+	—	—	+	+	—	0, ∞	—	NLA	Mana *et al.* (2013)
+	C	+	—	+	—	≤10	—	FEA	Gourvenec & Randolph (2003)
—	C	+	—	+	—	0, 6	—	LUB	Randolph & Puzrin (2003)
—	R	+	—	+	+	0	+ [d]	FEA	Gourvenec (2007a)
—	C	+	—	+	—	≤6	+	FEA	Gourvenec (2007b)
—	C	+	—		+	0	+	FEA	Taiebat & Carter (2010)
—	C		+	+	—	0, ∞	+	FEA	Zhang *et al.* (2011) [e]
—	C		+	+	—	0, 200	+	FEA	Vulpe *et al.* (2013) [e]
—	R [f]	+	+	+	—	0–200	+	FEA	Feng *et al.* (2014)
—	C	+	+	+	—	0–100	+	FEA	This study

[a]NLA, numerical limit analysis; FEA, finite-element analysis; LUB, lower and/or upper bound; EXP, experimental
[b]Spudcan foundations, failure envelopes tend to zero at low vertical loads
[c]Expression for HM space only
[d]Expression for no-tension soil–structure interface only
[e]Spudcan foundations
[f]Rectangular foundation, $B/L=0{\cdot}5$ only

Downloaded by [University Of Western Australia] on [15/11/15]. Copyright © ICE Publishing, all rights reserved.

and moment capacity factors and 3D failure envelopes as a function of foundation embedment ratio, normalised soil strength heterogeneity index and vertical load mobilisation, derived from 3D finite-element analyses (FEA).

FINITE-ELEMENT MODEL

Three-dimensional small-strain analyses were used to model the undrained capacity of shallow circular foundations under general VHM loading. The FEA were carried out using the commercial finite-element software Abaqus (Dassault Systèmes, 2012). Sign conventions for this study follow the recommendations of Butterfield *et al.* (1997) and the notation used in this study is defined in Table 2.

Model geometry and mesh

Circular foundations with embedment depth to diameter ratios d/D of 0 (surface), 0·10, 0·25 and 0·50 were considered. The foundations were wished-in-place (i.e. the installation process was not modelled). Zero-displacement boundaries of the mesh were located at a distance of $5D$ to either side of the foundation centreline and $5D$ below the free surface, sufficiently remote that the results were independent of the boundaries. Due to symmetry of the geometry and planar loading conditions, a semi-cylindrical section was modelled to optimise calculation efficiency. An example of the finite-element mesh used is shown in Fig. 1.

The soil was prescribed with first-order hexahedral hybrid elements. The foundation was modelled as a rigid body with a reference point for all loads and displacements prescribed on the axis of symmetry of the foundation at the base of the foundation (Fig. 2). The foundation was prescribed the same unit weight as the soil for geostatic equilibrium.

Material properties

The soil was modelled as a linear elastic–perfectly plastic material yielding according to the maximum shear stress, Tresca, failure criterion (i.e. $\tau_{max} = s_u$). Linearly increasing shear strength with depth was described by

$$s_u = s_{um} + kz \tag{1}$$

where s_{um} is the shear strength at the mudline and k is the shear strength gradient with depth z (Fig. 2).

The degree of soil strength heterogeneity can be normalised with the foundation diameter D through the dimensionless index

$$\kappa = \frac{kD}{s_{um}} \tag{2}$$

Values of κ of 0 (uniform shear strength with depth), 6, 20, 60 and 100 (essentially normally consolidated) were considered.

The soil was prescribed an undrained Young's modulus linearly increasing with depth with constant $E_u/s_u = 500$, Poisson's ratio $\nu = 0{\cdot}499$ and effective unit weight $\gamma' = 6$ kN/m^3, which are realistic values for a soft marine clay. The undrained ultimate limit state of a shallow foundation is independent of the magnitude of the elastic properties and self-weight of the soil (the strain or displacement to ultimate limit state is affected but not the magnitude of ultimate limit state), such that the particular values selected, while realistic, are incidental. The foundation–soil interface over the embedded portion of the foundation was fully bonded (i.e. fully rough in shear with no separation permitted).

Loading method

Load and displacement control were used to apply the combined load paths to the foundation. Pure vertical (V), horizontal (H) and moment (M) capacity were identified from displacement-controlled probes applied to the reference point until a plastic plateau was observed in the load–displacement response. General VHM loading was achieved by applying a vertical load as a direct force, after which a constant ratio displacement probe of translation and rotation was applied to the reference point. Vertical load level was defined as a proportion of the uniaxial vertical capacity, V_{ult}, described by $v = V/V_{ult}$, where v took values of 0, 0·50 or 0·75.

Validation

Vertical bearing capacity factors for the surface and embedded circular foundations predicted from the FEA were compared with exact solutions for the surface foundations (Martin, 2003) and upper bound solutions for the embedded cases (Martin & Randolph, 2001). Pure horizontal capacity of the surface foundation was compared with the theoretical solution for surface sliding ($H/As_u = 1$) and pure moment capacity was compared with a theoretical upper bound solution (Randolph & Puzrin, 2003). A mesh refinement study determined the optimum mesh discretisation as a function of soil strength heterogeneity index. The mesh refinement consisted of gradually increasing the number of elements around the foundation where the failure mechanism developed until further refinement did not improve the result. In some cases, a pragmatic assessment was made to tolerate a numerical over-prediction if the improvement in result was minimal but the addition of more elements caused an excessive increase in run time. For uniform strength with depth ($\kappa = 0$), the optimum mesh contained 35 000 elements, increasing to 50 000 elements for the case of $\kappa = 100$.

Vertical capacity of the surface foundation was accurately predicted for a range of soil strength heterogeneity, to within 1% of the theoretically exact solutions (Martin, 2003) and lower than the upper bound for the embedded foundation geometry (Martin & Randolph, 2001). Pure horizontal capacity of the surface foundations was close to the theoretical solution for surface sliding ($H/As_u = 1$) for a low strength heterogeneity index but was over-estimated with increasing degree of soil strength heterogeneity due to shearing in a single band of elements at the foundation–soil

Table 2. Definition of notation

	Vertical	Horizontal	Rotational
Displacement	w	u	θ
Load	V	H	M
Pure uniaxial capacity	V_{ult}	H_{ult}	M_{ult}
Maximum capacity	—	H_{max}	M_{max}
Normalised load	$v = V/V_{ult}$	$h = H/H_{ult}$	$m = M/M_{ult}$

Downloaded by [University Of Western Australia] on [15/11/15]. Copyright © ICE Publishing, all rights reserved.

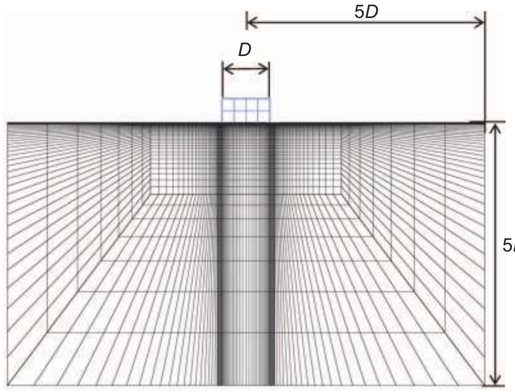

Fig. 1. Example of finite-element mesh ($d/D=0$)

interface (up to 10% for $\kappa=100$). Moment capacity was slightly over-predicted compared with a theoretical upper bound solution (Randolph & Puzrin, 2003), by up to 10%, due to representation of a circular scoop failure mechanism with hexahedral elements.

RESULTS

Pure vertical, horizontal and moment capacities (i.e. in the absence of other load components and referred to herein as uniaxial capacity), defined by V_{ult}, H_{ult} and M_{ult}, and combined vertical, horizontal and moment capacities of circular foundations with varying embedment ratio (d/D) and heterogeneity index ($\kappa=kD/s_{\text{um}}$) were quantified through over 1000 3D FEA. Capacity was defined as the mobilised resistance at which continued deformation occurred with no further increase in load (i.e. when the material response exhibited a plastic plateau). The results are presented through simple approximating formulae, enabling prediction of generalised failure envelopes for the extensive range of conditions considered.

Uniaxial capacity

It is convenient to consider the predicted uniaxial capacity in terms of depth factors d_{cV}, d_{cH} and d_{cM}, defined for a given degree of shear strength heterogeneity $\kappa=kD/s_{\text{um}}$. The depth factors are given by

$$d_{\text{cV}}=\frac{N_{\text{cV}(d/D,\kappa)}}{N_{\text{cV}(d/D=0,\kappa)}} \tag{3}$$

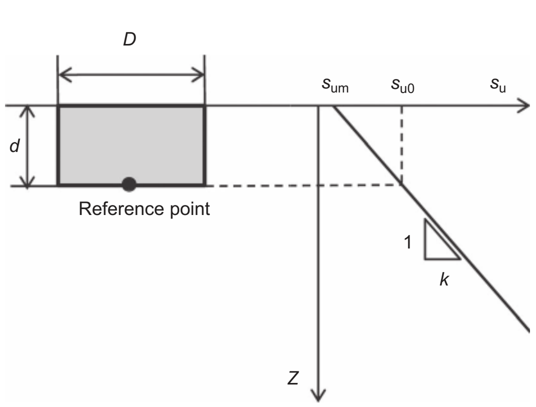

Fig. 2. Definition of notation for foundation geometry, reference point and soil strength profile

for vertical bearing capacity

$$d_{\text{cH}}=\frac{N_{\text{cH}(d/D,\kappa)}}{N_{\text{cH}(d/D=0,\kappa)}} \tag{4}$$

for horizontal capacity and

$$d_{cM}=\frac{N_{\text{cM}(d/D,\kappa)}}{N_{\text{cM}(d/D=0,\kappa)}} \tag{5}$$

for moment capacity. N_{cV}, N_{cH} and N_{cM} are the capacity factors defined by

$$N_{\text{cV}}=\frac{V_{\text{ult}}}{As_{\text{u0}}} \tag{6}$$

$$N_{\text{cH}}=\frac{H_{\text{ult}}}{As_{\text{u0}}} \tag{7}$$

$$N_{\text{cM}}=\frac{M_{\text{ult}}}{ADs_{\text{u0}}} \tag{8}$$

in which V_{ult}, H_{ult} and M_{ult} are the pure uniaxial capacities in the absence of other loading or restraint, A is the

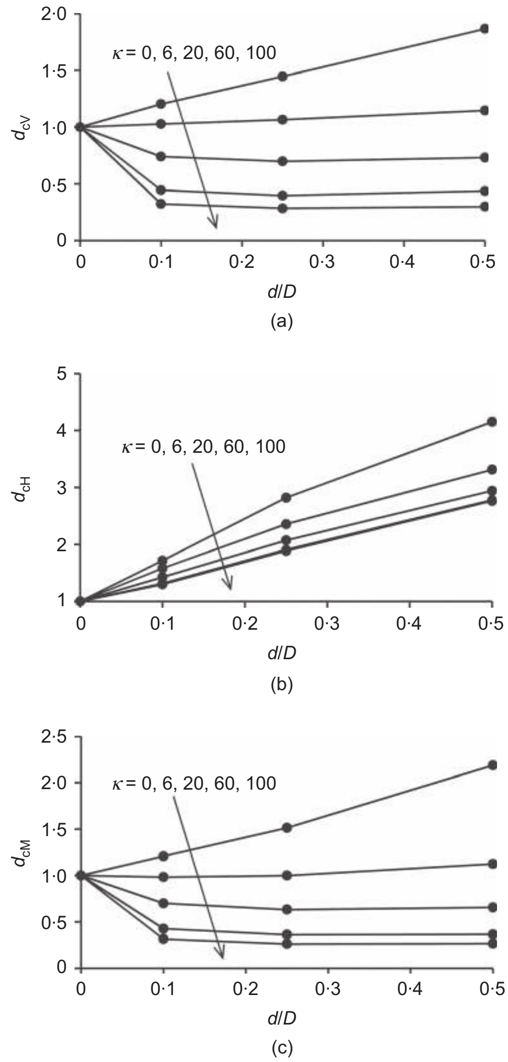

Fig. 3. Proposed depth factors for uniaxial loading: (a) vertical capacity; (b) horizontal capacity; (c) moment capacity

Downloaded by [University Of Western Australia] on [15/11/15]. Copyright © ICE Publishing, all rights reserved.

Table 3. Depth factors for uniaxial vertical, horizontal and moment capacity; $d_c = N_{c(d/D,\kappa)}/N_{c(d/D=0,\kappa)}$

d/D	$\kappa = kD/s_{um}$	d_{cV}	d_{cH}	d_{cM}
0	0	1	1	1
0	6	1	1	1
0	20	1	1	1
0	60	1	1	1
0	100	1	1	1
0·10	0	1·20	1·72	1·21
0·10	6	1·03	1·58	0·98
0·10	20	0·74	1·42	0·70
0·10	60	0·44	1·32	0·43
0·10	100	0·32	1·30	0·32
0·25	0	1·45	2·82	1·51
0·25	6	1·06	2·36	1·00
0·25	20	0·70	2·07	0·63
0·25	60	0·40	1·91	0·36
0·25	100	0·28	1·89	0·26
0·50	0	1·87	4·15	2·19
0·50	6	1·15	3·31	1·13
0·50	20	0·73	2·94	0·66
0·50	60	0·44	2·78	0·37
0·50	100	0·30	2·76	0·27

Table 4. Uniaxial capacity factors

d/D	$\kappa = kD/s_{um}$	N_{cV}	N_{cH}	N_{cM}
0	0	6·05	1	0·67
0	6	9·85	1	1·19
0	20	15·48	1	1·92
0	60	27·69	1	3·49
0	100	37·88	1	4·77
0·10	0	7·28	1·72	0·81
0·10	6	10·11	1·58	1·17
0·10	20	11·46	1·42	1·35
0·10	60	12·30	1·32	1·49
0·10	100	12·25	1·30	1·50
0·25	0	8·75	2·82	1·01
0·25	6	10·48	2·36	1·19
0·25	20	10·81	2·07	1·22
0·25	60	10·97	1·91	1·26
0·25	100	10·78	1·89	1·25
0·50	0	11·29	4·15	1·47
0·50	6	11·29	3·31	1·34
0·50	20	11·31	2·94	1·26
0·50	60	12·07	2·78	1·28
0·50	100	11·31	2·76	1·27

cross-sectional plan area of the foundation, D is the foundation diameter and s_{u0} is the undrained shear strength at foundation level, $s_{u0} = s_{um} + kd$.

The vertical bearing capacity factor $N_{cV(d/D=0,\kappa)}$ for a surface circular foundation (i.e. $d/D=0$) can be defined as a function of soil strength heterogeneity index κ from

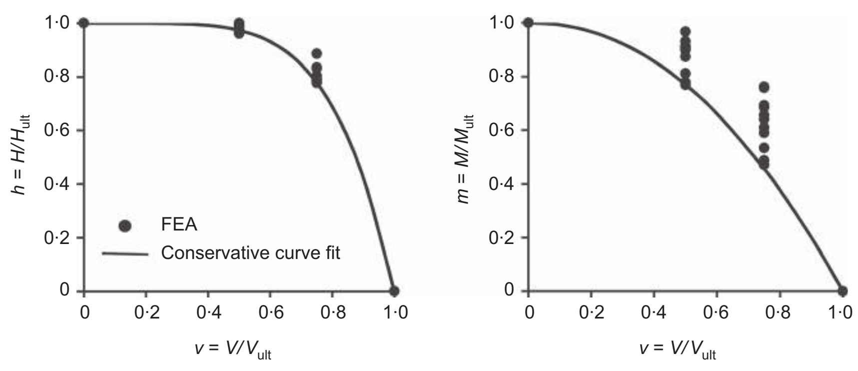

Fig. 4. Definition of lower limit to normalised vh and vm interactions over range of d/D and κ

Downloaded by [University Of Western Australia] on [15/11/15]. Copyright © ICE Publishing, all rights reserved.

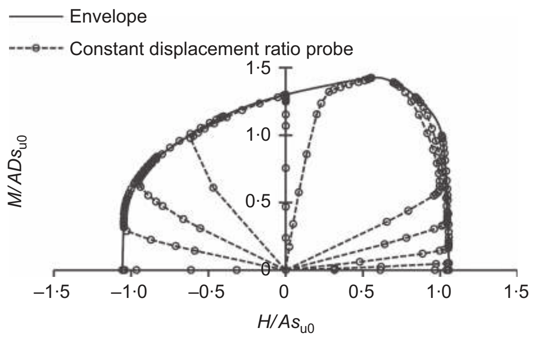

Fig. 5. Example of failure envelope using probe tests from FEA (d/D=0, κ=6, V=0)

available exact analytical solutions for a limited range of κ (Houlsby & Wroth, 1983), from numerical solutions (Gourvenec & Mana, 2011) or with the numerical limit analysis freeware ABC (Martin, 2003). The various sources result in a similar relationship, which can be approximated through

$$F_{\mathrm{V}} = \frac{N_{\mathrm{cV}(d/D=0,\kappa)}}{N_{\mathrm{cV}(d/D=0,\kappa=0)}} = 1 + (0{\cdot}09\kappa)^{0{\cdot}76} \tag{9}$$

where $N_{\mathrm{cV}(d/D=0,\kappa=0)}$ =6·05, the exact solution for a rough circular foundation on Tresca material (Cox *et al.*, 1961).

$N_{\mathrm{cH}(d/D=0,\kappa)}$ =1 irrespective of the soil heterogeneity index since the pure horizontal load capacity of a surface foundation is governed by the mudline shear strength for cases of uniform or increasing shear strength with depth.

$N_{\mathrm{cM}(d/D=0,\kappa)}$ can be defined as a function of soil strength heterogeneity coefficient from the FEA solutions as

$$F_{\mathrm{M}} = \frac{N_{\mathrm{cM}(d/D=0,\kappa)}}{N_{\mathrm{cM}(d/D=0,\kappa=0)}} = 1 + 0{\cdot}21\kappa^{0{\cdot}74} \tag{10}$$

where $N_{\mathrm{cM}(d/D=0,\kappa=0)}$ =0·67, from an upper bound solution (Randolph & Puzrin, 2003).

The depth factors for pure vertical, horizontal and moment capacity of circular foundations with embedment ratio $0 \leq d/D \leq 0{\cdot}50$ and soil shear strength heterogeneity index $0 \leq \kappa \leq 100$ are shown in Fig. 3 and summarised in Table 3. Uniaxial capacity factors derived from Table 3 and equations (3)–(10) are summarised in Table 4 to allow for direct interpolation of uniaxial ultimate limit states V_{ult}, H_{ult} and M_{ult}.

Combined vertical and horizontal load (VH) and vertical load and moment (VM) capacity

Ultimate limit states under combined vertical and horizontal load and vertical load and moment are shown in Fig. 4 for the range of embedment ratios and soil strength heterogeneity considered in normalised vh and vm space, where $v=V/V_{\mathrm{ult}}$, $h=H/H_{\mathrm{ult}}$ and $m=M/M_{\mathrm{ult}}$. A power law expression is used to define a lower limit of normalised vh and vm interaction; that is, the FE results for all embedment ratios and degrees of soil strength heterogeneity fall outside the fitted curve.

The normalised failure envelopes in vh space are closely banded, irrespective of the foundation embedment ratio or the soil shear strength heterogeneity index. The distribution of failure envelopes in normalised vm space is more diverse but shows no clear trend for grouping by embedment ratio or shear strength heterogeneity. Conservative fits to the vh and vm interactions are given by the power laws

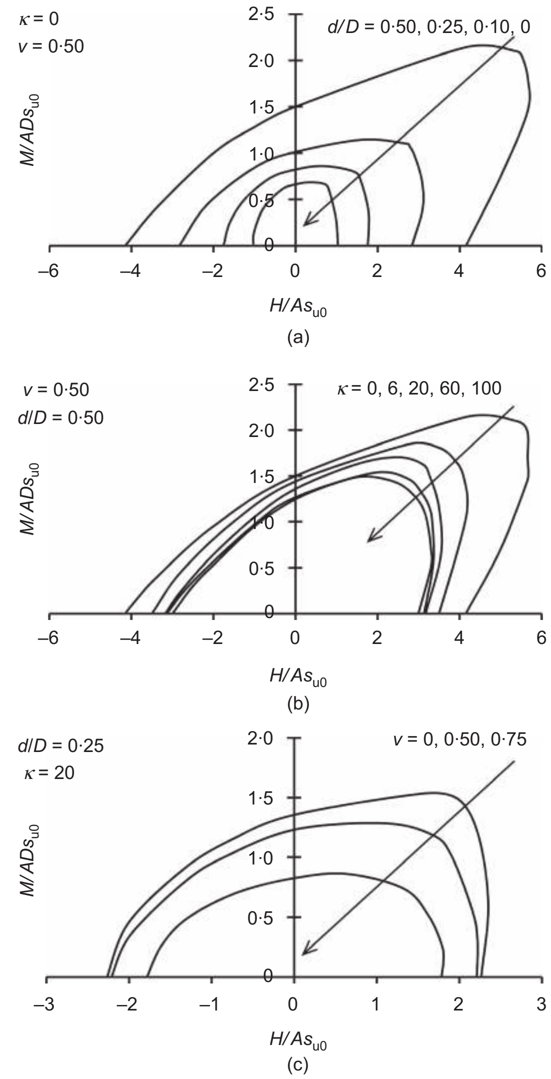

Fig. 6. Effect on shape and size of VHM failure envelopes of varying (a) foundation embedment ratio d/D, (b) soil strength heterogeneity index, $\kappa=kD/s_{\mathrm{um}}$ and (c) vertical load mobilisation $v=V/V_{\mathrm{ult}}$

$$h^* = 1 - v^q \tag{11}$$

where q=4·69 and

$$m^* = 1 - v^p \tag{12}$$

in which p=2·12.

The expressions h^* and m^* are functions used to describe the interactions in vh and vm space and determine the limiting horizontal or moment load in conjunction with a known applied vertical load. Inference of displacements at failure through the principle of normality should not be applied to the bounding surfaces described by equations (11) and (12) since they simply represent a lower limit to a range of observed results for a range of boundary conditions, rather than the precise shape of a particular failure envelope for a given set of boundary conditions. A failure envelope observing normality would be expected to exhibit zero change of gradient across the H = 0 or M=0 axes.

Vertical, horizontal and moment (VHM) capacity

Failure envelopes were constructed in HM load space by interpolating between individual HD/M load paths resulting

Downloaded by [University Of Western Australia] on [15/11/15]. Copyright © ICE Publishing, all rights reserved.

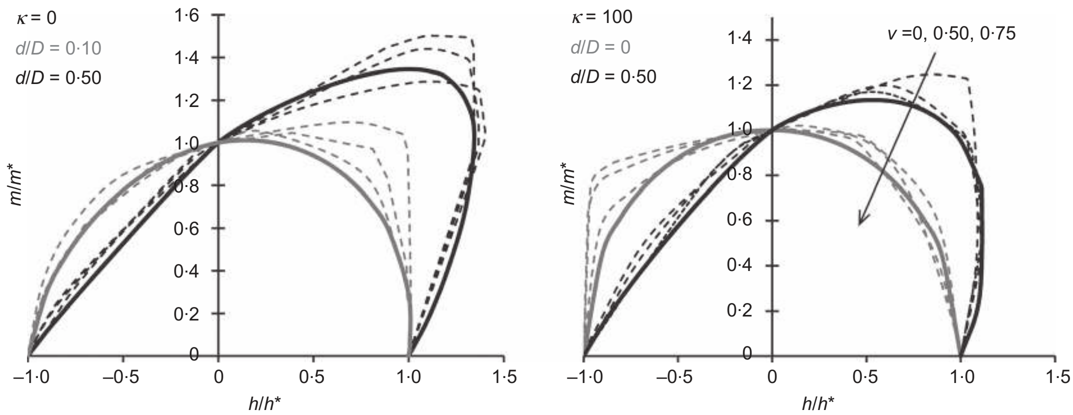

Fig. 7. Comparison of selected failure envelopes predicted by FEA (broken lines) and approximating expression (solid lines) (equation (13)); applicable to all levels of vertical load mobilisation V/V_{ult}

Table 5. Fitting parameters for approximating expression for VHM envelope for vertical load mobilisation $0 \leq V/V_{ult} \leq 1$

κ	α				β			
	d/D				d/D			
	0	0·10	0·25	0·50	0	0·10	0·25	0·50
0	1·63	1·93	2·16	1·61	−0·05	−0·16	−0·44	−0·60
6	2·00	1·85	1·94	1·76	0·06	−0·10	−0·27	−0·55
20	2·46	2·09	1·90	1·99	−0·01	−0·02	−0·21	−0·48
60	2·89	2·12	1·99	2·02	0·13	0·02	−0·24	−0·46
100	3·12	2·05	2·00	1·65	0·13	0·00	−0·22	−0·48

Table 6. Values of h_{max}/h^* for vertical load mobilisation $0 \leq V/V_{ult} \leq 1$

d/D	κ				
	0	6	20	60	100
0	1	1	1	1	1
0·10	1	1	1	1	1
0·25	1·09	1·02	1·01	1	1
0·50	1·35	1·15	1·13	1·11	1·11

Table 7. Fitting parameters for approximating expression for VHM envelope for limited vertical load mobilisation $V/V_{ult} \leq 0{\cdot}50$

κ	α				β			
	d/D				d/D			
	0	0·10	0·25	0·50	0	0·10	0·25	0·50
0	2·13	2·33	2·33	1·46	−0·26	−0·28	−0·49	−0·57
6	2·58	2·09	2·10	1·76	−0·11	−0·23	−0·35	−0·55
20	2·83	2·47	2·01	1·83	−0·03	−0·15	−0·29	−0·55
60	3·32	2·51	2·10	2·19	0·04	−0·13	−0·29	−0·51
100	3·74	2·56	2·12	1·90	0·08	−0·12	−0·27	−0·48

Table 8. Maximum values of h_{max}/h^* for low vertical load mobilisation $V/V_{ult} \leq 0{\cdot}50$

d/D	κ				
	0	6	20	60	100
0	1	1	1	1	1
0·10	1·01	1	1	1	1
0·25	1·09	1·01	1·01	1	1
0·50	1·34	1·15	1·11	1·10	1·10

Downloaded by [University Of Western Australia] on [15/11/15]. Copyright © ICE Publishing, all rights reserved.

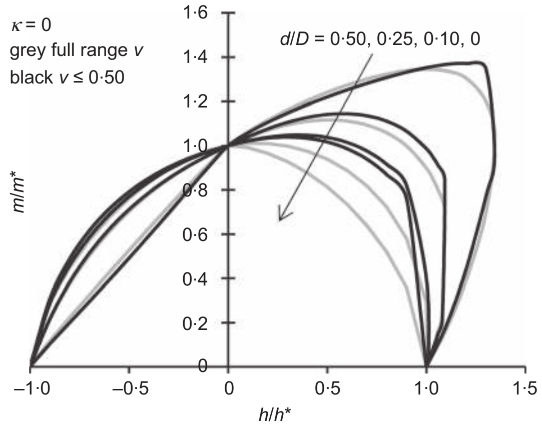

Fig. 8. Effect of vertical load mobilisation on available combined load capacity for full range of v (grey lines) and $v<0{\cdot}50$ (black lines)

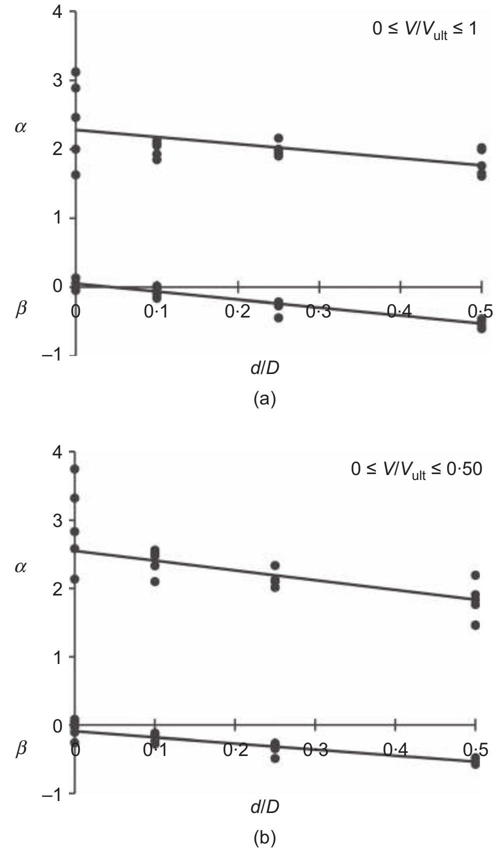

Fig. 9. Simplified fitting parameters α_{av} and β_{av} (lines) and exact fitting parameters (symbols)

from constant ratio displacement probes ($u/D\theta$), as illustrated in Fig. 5. Once the failure envelope is reached, each load path travels around the envelope until it reaches a point where the normal to the failure envelope corresponds to the prescribed displacement ratio.

Figure 6 shows two dimensional slices in the HM plane through 3D VHM failure envelopes in dimensionless load space (H/As_{u0}, M/ADs_{u0}) at discrete levels of vertical load mobilisation $v = V/V_{ult}$. The failure envelopes in HM load space are seen to be asymmetrical about the H and M axes. The degree of asymmetry depends on the load combination, foundation embedment ratio and soil strength heterogeneity and has been observed both experimentally (Gottardi *et al.*, 1999; Martin & Houlsby, 2000; Zhang *et al.*, 2014) and numerically (Ukritchon *et al.*, 1998; Bransby & Randolph, 1999; Martin & Houlsby, 2001; Gourvenec & Randolph, 2003; Gourvenec, 2008; Bransby & Yun, 2009; Zhang *et al.*, 2011).

The selections of FEA results presented in Fig. 6 demonstrate the effect on the size and shape of the failure envelopes with varying foundation embedment ratio (Fig. 6(a)), soil shear strength heterogeneity coefficient (Fig. 6(b)) and relative vertical load level (Fig. 6(c)). The results shown in Fig. 5 are consistent with the 60 sections of HM envelopes generated across the full range of foundation and soil conditions considered and are selected to illustrate the observed trends, avoiding the clutter of presentation of all results.

Embedment ratio and soil strength heterogeneity have the greatest influence on the shape of the failure envelopes (Figs 6(a) and 6(b), while the influence of the level of vertical load mobilisation is secondary (Fig. 6(c)). Increasing obliqueness of the failure envelopes (due to HM cross-coupling) is associated with increasing embedment ratio while asymmetry about the moment axis is associated with reducing soil strength heterogeneity. The level of vertical load has, by comparison, only secondary effects on the shape of the failure envelopes.

APPROXIMATING EXPRESSION

An approximating expression to predict the shape of the normalised VHM failure envelopes as a function of foundation embedment ratio and soil strength heterogeneity index can be defined by the elliptical expression

$$\left(\left|\frac{h}{h^*}\right|\right)^{\alpha} + \left(\frac{m}{m^*}\right)^{\alpha} + 2\beta\frac{hm}{h^*m^*} = 1 \tag{13}$$

in which $h = H/H_{ult}$ and $m = M/M_{ult}$ define the normalised horizontal load and moment mobilisation, while the effect of vertical mobilisation, $v = V/V_{ult}$, is taken into account through h^* and m^* (equations (11) and (12)). α and β are fitting parameters that depend on the foundation embedment ratio and soil shear strength heterogeneity index. In this case, the effect of the level of vertical load mobilisation is neglected in the prediction of the shape of the failure envelope (since the influence is considered secondary), but is incorporated in the prediction of the size of the failure envelope through h^* and m^*. The form of equation (13) was proposed by Gourvenec & Barnett (2011) for embedded strip foundations, but was defined as a function of embedment ratio only, since only low values of soil strength heterogeneity were considered in that case ($\kappa \leq 6$) and therefore the effect was limited.

Figure 7 compares FEA results with the approximating expression in normalised h^*m^* space for selected values of the foundation embedment ratio and soil strength heterogeneity index. The FEA capture the changing shape of the failure envelopes.

The fitting parameters α and β are listed in Table 5. Fitting parameters can be interpolated for intermediate values of the foundation embedment ratio and shear strength heterogeneity index. The values of h_{max}/h^* (h_{max} represents the maximum horizontal mobilisation as a result of HM cross-coupling) required to reconstruct the failure envelopes are given in Table 6.

The results presented in Fig. 7 indicate that the approximating expression becomes increasingly conservative for low vertical mobilisation $v = V/V_{ult}$ by neglecting the effect of vertical load level, but captures changes in shape associated with the foundation embedment ratio and soil strength heterogeneity. It should be borne in mind that predictions of ultimate limit states under combined loading

Downloaded by [University Of Western Australia] on [15/11/15]. Copyright © ICE Publishing, all rights reserved.

Table 9. Summary of proposed procedure

Step	Activity	Reference
1	Evaluate d/D, s_{u0} and kD/s_{um} for given foundation geometry and soil strength profile	
2	Calculate F_v, d_{cV}, N_{cV} and V_{ult}	Equations (9), (3) and (6)
3	Calculate vertical utilisation ratio $v = V/V_{ult}$	—
4	Calculate h^* and m^*	Equations (11) and (12)
5	Choose exact fitting parameters α and β or calculate average fitting parameters α_{av} and β_{av}	Tables 5 and 7, Equations (14) and (15)
6	Plot normalised h^*m^* envelope for given v (for constant intervals of h solve for m)	—
7	Calculate N_{cH} and N_{cM} (in absence of other loads or constraints)	Equations (10), (4), (5), (7) and (8)
8	Calculate H^*/As_{u0} and M^*/ADs_{u0} at given vertical load level (i.e. h^* and m^* multiplied by N_{cH} and N_{cM}, respectively)	—
9	Convert h^*m^* envelope to dimensionless load space (i.e. $h/(H^*/As_{u0})$ and $m/(M^*/ADs_{u0})$)	—

from the approximating expression proposed here are considerably less conservative than the predictions resulting from methods based on classical bearing capacity theory (demonstrated explicitly by Ukrtichon *et al.* (1998) and Gourvenec & Barnett (2011)), which forms the basis of industry design guidance worldwide.

For cases in which vertical loads are known to be well below vertical capacity, optimised values of the fitting parameters α and β were derived for low values of vertical load mobilisation. Optimised fitting parameters for vertical load mobilisation $v = V/V_{ult} \leq 0{\cdot}50$ are presented in Table 7, with the necessary values of h_{max}/h^* to reconstruct the envelopes given in Table 8. Figure 8 illustrates the potential efficiency of accounting for limited vertical load mobilisation, showing larger normalised failure envelopes for the cases of limited vertical load mobilisation.

Simplified fitting parameters defined as a function of only the embedment ratio can be used to give a quick, rough indication of the failure envelope. For $0 \leq V/V_{ult} \leq 1$, representative fitting parameters may be given by

$$\alpha_{av} = 2{\cdot}28 - 1{\cdot}03(d/D) \tag{14a}$$

$$\beta_{av} = 0{\cdot}05 - 1{\cdot}15(d/D) \tag{14b}$$

and for low vertical load mobilisation, $V/V_{ult} \leq 0{\cdot}50$, by

$$\alpha_{av} = 2{\cdot}55 - 1{\cdot}43(d/D) \tag{15a}$$

$$\beta_{av} = -0{\cdot}09 - 0{\cdot}88(d/D) \tag{15b}$$

Figures 9(a) and 9(b) show that α and β are closely banded for each embedment ratio, except for the surface case, irrespective of soil strength heterogeneity and that the averaged expressions for α_{av} and β_{av} (equations (14) and (15)) provide a satisfactory fit.

The procedure for recreating a failure envelope for a given foundation embedment ratio, soil strength heterogeneity index and vertical load mobilisation based on the method proposed in this paper is outlined in Table 9.

CONCLUDING REMARKS

This paper has presented undrained uniaxial ultimate limit states and failure envelopes for the VHM capacity of shallow circular foundations across a practical range of foundation embedment ratio and soil strength heterogeneity index. The shape of the normalised failure envelope is shown to vary with foundation embedment ratio and soil strength heterogeneity index and, to a lesser extent, with the level of vertical load mobilisation. A single algebraic expression was proposed to approximate failure envelopes as a function of embedment ratio and soil strength heterogeneity index. Fitting parameters for conditions of limited vertical load mobilisation were also proposed. Uniaxial bearing capacity factors were proposed through depth factors to transform normalised failure envelopes to absolute load space.

The tabulated data and fitting expressions proposed in the paper can be incorporated into a spreadsheet to

- enable automatic calculation of failure envelopes for selected foundation geometries and shear strength profiles
- optimise foundation geometry for a given set of design loads and shear strength profile
- evaluate load or material factors.

ACKNOWLEDGEMENTS

This work forms part of the activities of the Centre for Offshore Foundation Systems (COFS), currently supported as a node of the Australian Research Council Centre of Excellence for Geotechnical Science and Engineering. The work presented in this paper is supported through ARC grant (DP140100684), which is gratefully acknowledged.

REFERENCES

Bransby, M. F. & Randolph, M. F. (1998). Combined loading of skirted foundations. *Géotechnique* **48**, No. 5, 637–655.

Bransby, M. F. & Randolph, M. F. (1999). The effect of embedment depth on the undrained response of skirted foundations to combined loading. *Soils and Found.* **39**, No. 4, 19–33.

Bransby, M. F. & Yun, G. J. (2009). The undrained capacity of skirted strip foundations under combined loading. *Géotechnique* **59**, No. 2, 115–125.

Butterfield, R. & Gottardi, G. (1994). A complete three dimensional failure envelope for shallow footings on sand. *Géotechnique* **44**, No. 1, 181–184.

Butterfield, R. & Ticof, J. (1979). Design parameters for granular soils (discussion contribution). *Proc. 7th European Conf. Soil Mech. and Foundation Engng (ECSMFE), Brighton*, **4**, 259–261.

Butterfield, R., Houlsby, G. T. & Gottardi, G. (1997). Standardised sign conventions and notation for generally loaded foundations. *Géotechnique* **47**, No. 4, 1051–1052.

Cox, A. D., Eason, G. & Hopkins, H. G. (1961). Axially symmetric plastic deformation in soils. *Proc. Royal Soc. London, Ser. A* **254**, 1–45.

Dassault Systèmes (2012). *Abaqus analysis user's manual*. Providence, RI: Simulia Corp.

Feng, X., Randolph, M. F., Gourvenec, S. & Wallerand, R. (2014). Design approach for rectangular mudmats under fully three dimensional loading, *Géotechnique* **64**, No. 1, 51–63.

Downloaded by [University Of Western Australia] on [15/11/15]. Copyright © ICE Publishing, all rights reserved.

Gottardi, G. & Butterfield, R. (1993). On the bearing capacity of surface footings on sand under general planar load. *Soils and Found.* **33**, No. 3, 68–79.

Gottardi, G., Houlsby, G. T. & Butterfield, R. (1999). Plastic response of circular footings on sand under general planar loading. *Géotechnique* **49**, No. 4, 453–469.

Gourvenec, S. (2007a). Failure envelopes for offshore shallow foundations under general loading. *Géotechnique* **57**, No. 3, 715–728.

Gourvenec, S. (2007b). Shape effects on the capacity of rectangular footings under general loading. *Géotechnique* **57**, No. 8, 637–646.

Gourvenec, S. (2008). Effect of embedment on the undrained capacity of shallow foundations under general loading. *Géotechnique* **58**, No. 3, 177–185.

Gourvenec, S. & Barnett, S. (2011). Undrained failure envelope for skirted foundations under general loading. *Géotechnique* **61**, No. 3, 263–270.

Gourvenec, S. & Mana, D. K. S. (2011). Undrained vertical bearing capacity factors for shallow foundations. *Géotechnique Lett*. **1**, No. 4, 101–108.

Gourvenec, S. & Randolph, M. F. (2003). Effect of strength non-homogeneity on the shape and failure envelopes for combined loading of strip and circular foundations on clay. *Géotechnique* **53**, No. 6, 575–586.

Govoni, L., Gourvenec, S. & Gottardi, G. (2011). A centrifuge study on the effect of embedment on the drained response of shallow foundations under combined loading. *Géotechnique* **61**, No. 12, 1055–1068.

Houlsby, G. T. & Wroth, C. P. (1983). Calculation of stresses on shallow penetrometers and footings. *Proc. IUTAM/IUGG Seabed Mechanics, Newcastle*, 107–112.

Mana, D. K. S., Gourvenec, S. & Martin, C. M. (2013). Critical skirt spacing for shallow foundations under general loading. *ASCE J. Geotech. Geoenviron. Engng* **139**, No. 9, 1554–1566.

Martin, C. M. (2003). New software for rigorous bearing capacity calculations. *Proc. Br. Geotech. Assoc. Int. Conf. on Foundations, Dundee*, 581–592.

Martin, C. M. & Houlsby, G. T. (2000). Combined loading of spudcan foundations on clay: laboratory tests. *Géotechnique* **50**, No. 4, 325–338.

Martin, C. M. & Houlsby, G. T. (2001). Combined loading of spudcan foundations on clay: numerical modelling. *Géotechnique* **51**, No. 8, 687–699.

Martin, C. M. & Randolph, M. F. (2001). Applications of the lower and upper bound theorems of plasticity to collapse of circular foundations. *Proc. 10th Int. Conf. Int. Assoc. of Computer Methods and Advances in Geomech (IACMAG), Tucson* **2**, 1417–1428.

Meyerhof, G. G. (1953). The bearing capacity of foundations under eccentric and inclined loads. *Proc. 3rd Int. Conf. on Soil Mechanics and Foundation Engng, Zurich, Switzerland*, **1**, 440–445.

Nova, R. & Montrasio, L. (1991). Settlements of shallow foundations on sand. *Géotechnique* **41**, No. 2, 243–256.

Randolph, M. F. & Puzrin, A. M. (2003). Upper bound limit analysis of circular foundations on clay under general loading. *Géotechnique* **53**, No. 9, 785–796.

Roscoe, K. H. & Schofield, A. N. (1957). The stability of short pier foundations in sand: discussion. *Br. Weld. J.*, January, 12–18.

Taiebat, H. A. & Carter, J. P. (2000). Numerical studies of the bearing capacity of shallow foundations on cohesive soil subjected to combined loading. *Géotechnique* **50**, No. 4, 409–418.

Taiebat, H. A. & Carter, J. P. (2010). A failure surface for shallow circular footings on cohesive soils. *Géotechnique* **60**, No. 4, 265–273.

Ukritchon, B., Whittle, A. J. & Sloan, S. W. (1998). Undrained limit analysis for combined loading of strip footings on clay. *ASCE J. Geotech. Geoenviron. Engng* **124**, No. 3, 265–276.

Vulpe, C., Bienen, B. & Gaudin, C. (2013). Predicting the undrained capacity of skirted spudcans under combined loading. *Ocean Engng* **74**, 178–188.

Yun, G. & Bransby, M. F. (2007). The horizontal-moment capacity of embedded foundations in undrained soil. *Can. Geotech. J.* **44**, No. 4, 409–427.

Zhang, Y., Bienen, B., Cassidy, M.J. & Gourvenec, S. (2011). The undrained bearing capacity of a spudcan foundation under combined loading in soft clay. *Marine Struct*. **24**, No. 4, 459–477.

Zhang, Y., Bienen, B., & Cassidy, M. J. (2014). A plasticity model for spudcan foundations in soft clay. *Can. Geotech. J.* **51**, No. 6, 629–646, http://dx.doi.org/10.1139/cgj-2013-0269.

WHAT DO YOU THINK?

To discuss this paper, please email up to 500 words to the editor at journals@ice.org.uk. Your contribution will be forwarded to the author(s) for a reply and, if considered appropriate by the editorial panel, will be published as a discussion.

Downloaded by [University Of Western Australia] on [15/11/15]. Copyright © ICE Publishing, all rights reserved.